

Supplementary Methods

Pharmacokinetics

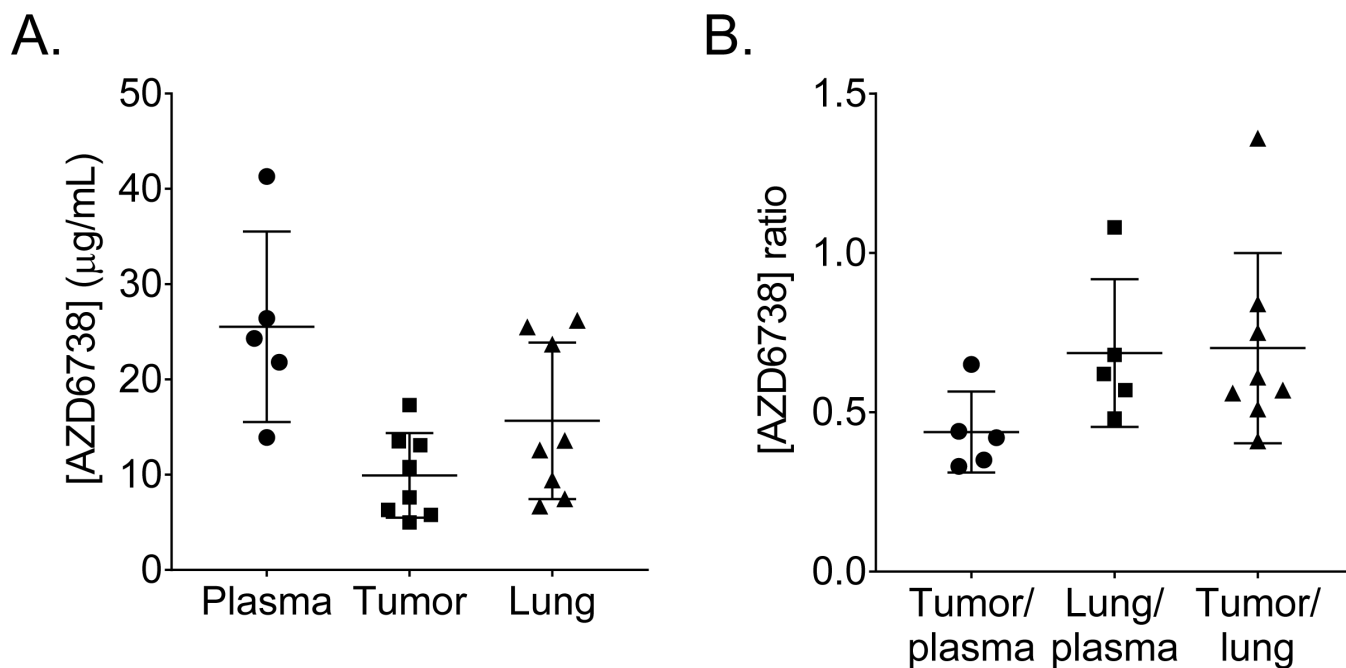
CT26 tumor-bearing BALB/c mice received a single, 75 mg/kg oral dose of AZD6738. At 40 minutes after dosing, mice were euthanized and whole blood (via cardiac puncture), lung, and tumor were harvested. Whole blood was processed to obtain plasma. Quantitation of AZD6738 in tissues was performed as previously described (1).

CD8 depletion pilot experiments

For validation of CD8 depletion, non-tumor bearing BALB/c mice were administered anti-CD8 antibody (α CD8, 250 μ g) or vehicle (1x PBS) by intraperitoneal injection on days 1 and 4 or days 1-2, and spleens were harvested at day 8 or day 5, respectively. Spleens were processed and stained with anti-CD45 BV785, anti-CD4 BV650, anti-CD8 BB515, and eFluor780 viability dye as described in the main methods. Flow cytometry acquisition and data analyses were performed as described in the main methods. For assessing the impact of CD8 depletion on growth of CT26 tumors, BALB/c mice were injected subcutaneously in the right hind flank with 5×10^5 CT26 cells in RPMI. Once tumors reach approximately 60-90 mm³, mice were administered anti-CD8 antibody (α CD8, 250 μ g) or vehicle (1x PBS) by intraperitoneal on days 1, 4, and 8, or on days 1-2, and tumor growth was measured twice weekly.

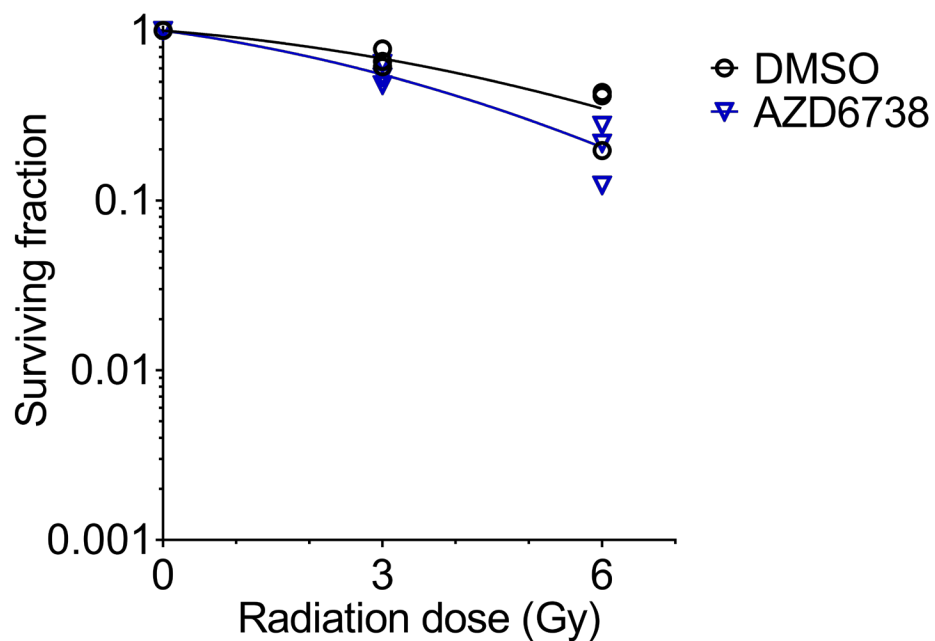
PD-L1 knockout CT26 cells

A PD-L1 knockout (KO) CT26 cell line was generated using CRISPR-Cas9 mediated genome editing with guide RNAs were purchased from GenScript. PE-conjugated anti-PD-L1 antibody (clone 10F.9G2) or IgG2b κ isotype control antibody (clone RTK4530), both purchased from BioLegend and used at a concentration of 1:100, were used to validated knockout of PD-L1 by loss of cell surface PD-L1 expression by flow cytometry. Analyses were performed using an Accuri C6 cytometer (BD Biosciences) with slow flow rate (14 μ L/min) and CFlow software. To assess growth of PD-L1 KO CT26 cells *in vivo*, BALB/c mice were injected subcutaneously in the right hind flank with 1.3×10^6 CT26 cells in RPMI and tumor growth was measured over time.



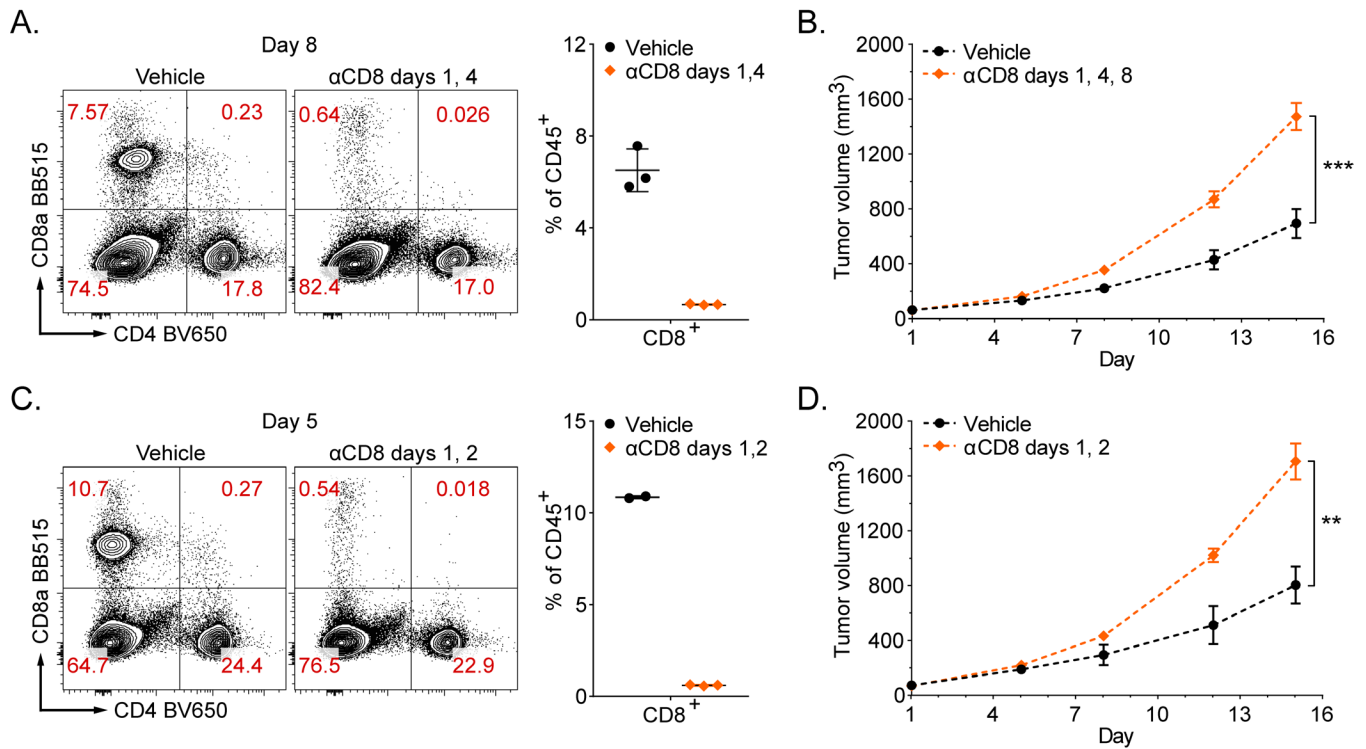
Supplementary Figure S1. Pharmacokinetics of AZD6738 at the time of radiation.

A. Concentrations of AZD6738 in the plasma, lungs, and tumors of CT26 tumor-bearing BALB/c mice at 40 minutes after a single, 75 mg/kg, oral dose. $n = 8$ mice ($n = 5$ plasma samples analyzed). **B.** Ratios of the concentration of AZD6738 in tumor and lung relative to plasma, and tumor relative to lung. Mean and SD bars shown.



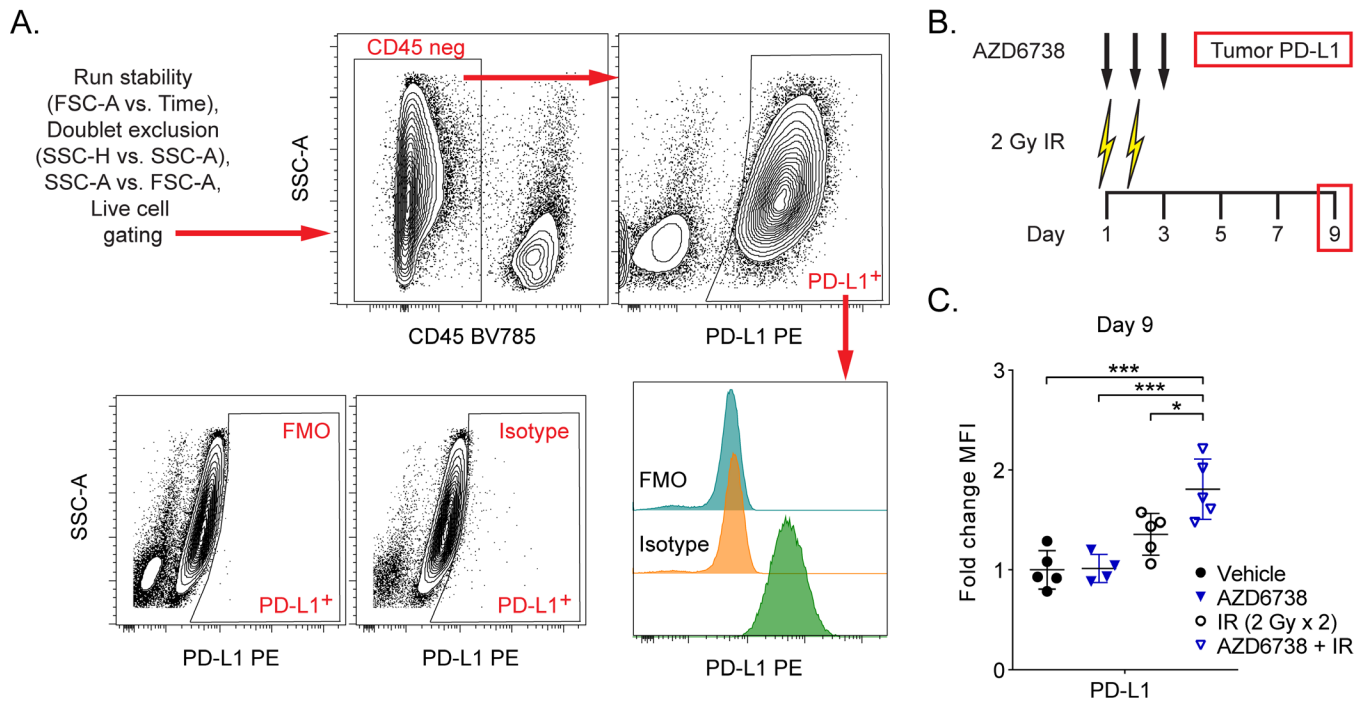
Supplementary Figure S2. AZD6738 does not radiosensitize CT26 cells *in vitro*.

Clonogenic survival of CT26 cells treated *in vitro* with 3 Gy and 6 Gy IR and 300 nM AZD6738 or DMSO. Data were plotted as the surviving fraction normalized to 0 Gy controls within a given treatment, and curves were fitted using the linear quadratic model. Each data point represents the mean of 3 technical replicates within a given experiment. $n = 3$ independent experiments. Two-tailed unpaired t-test determined no statistically significant differences between AZD6738 and DMSO at either dose of radiation.



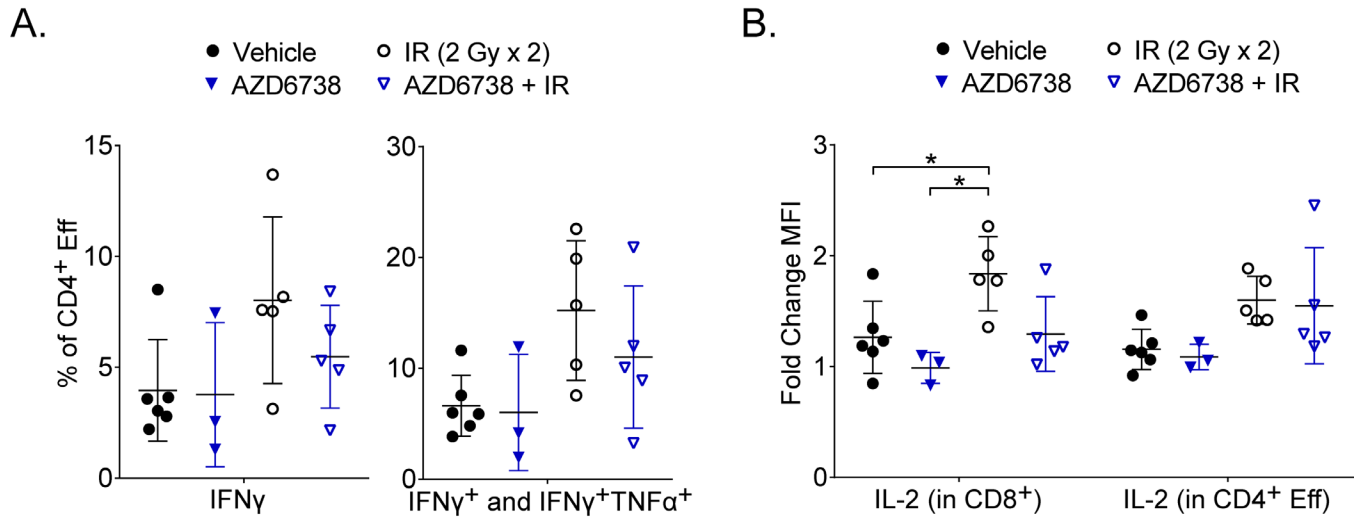
Supplementary Figure S3. Depletion of CD8⁺ T cells accelerates growth of syngeneic CT26 tumors.

A. Validation of CD8 depletion in non-tumor bearing BALB/c mice following administration of anti-CD8 antibody (αCD8, 250 μg) or vehicle on days 1 and 4. Shown are representative contour plots and corresponding quantitation (as a percentage of CD45⁺ immune cells) of splenic CD8⁺ T cells at day 8. n per arm (mice) = 3. Mean and SD bars shown. **B.** CT26 tumor bearing BALB/c mice were administered αCD8 (250 μg) or vehicle on days 1, 4, and 8, and tumor growth was followed over time. Data represent mean tumor volumes ± SEM. n per arm (mice) = 5. ***p<0.001 by unpaired, two-tailed t-test for αCD8 vs. vehicle at day 15. **C.** Validation of CD8 depletion in non-tumor bearing BALB/c mice following administration of αCD8 (250 μg) or vehicle on days 1-2. Shown are representative contour plots and corresponding quantitation (as a percentage of CD45⁺ immune cells) of splenic CD8⁺ T cells at day 5. n per arm (mice) = 2 Vehicle, 3 αCD8. Mean and SD bars shown. **D.** CT26 tumor bearing BALB/c mice were administered αCD8 (250 μg) or vehicle on days 1-2, and tumor growth was followed over time. Data represent mean tumor volumes ± SEM. n per arm (mice) = 3 Vehicle, 4 αCD8. **p<0.01 by unpaired, two-tailed t-test for αCD8 vs. vehicle at day 15.



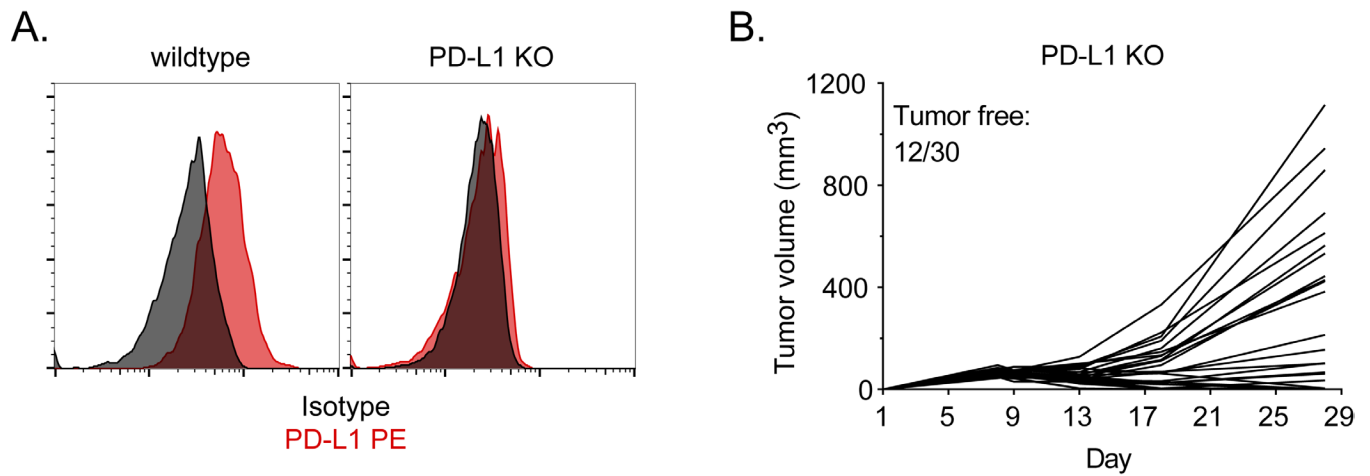
Supplementary Figure S4. Cell surface expression of PD-L1 in CT26 tumors following treatment with AZD6738 and radiation.

A. Gating strategy to determine cell surface expression of PD-L1 (as measured by median fluorescence intensity) on live, CD45 negative, CT26 tumor cells. Fluorescence minus one (FMO, no PD-L1) and isotype controls also shown **B.** Schematic showing schedules of IR and AZD6738 treatments and day 9 time point for PD-L1 expression analysis. **C.** Quantitation of the fold-change in PD-L1 median fluorescence intensity (MFI) at day 9 relative to the average MFI of Vehicle control tumors (within a given experiment). Data from 2 independent experiments, each with 2-3 mice per arm. n = 5 Vehicle, 4 AZD6738, 5 IR, 5 AZD6738 + IR. Mean and SD bars shown. * $p < 0.05$, *** $p < 0.001$ by ANOVA with Tukey's multiple comparisons test.



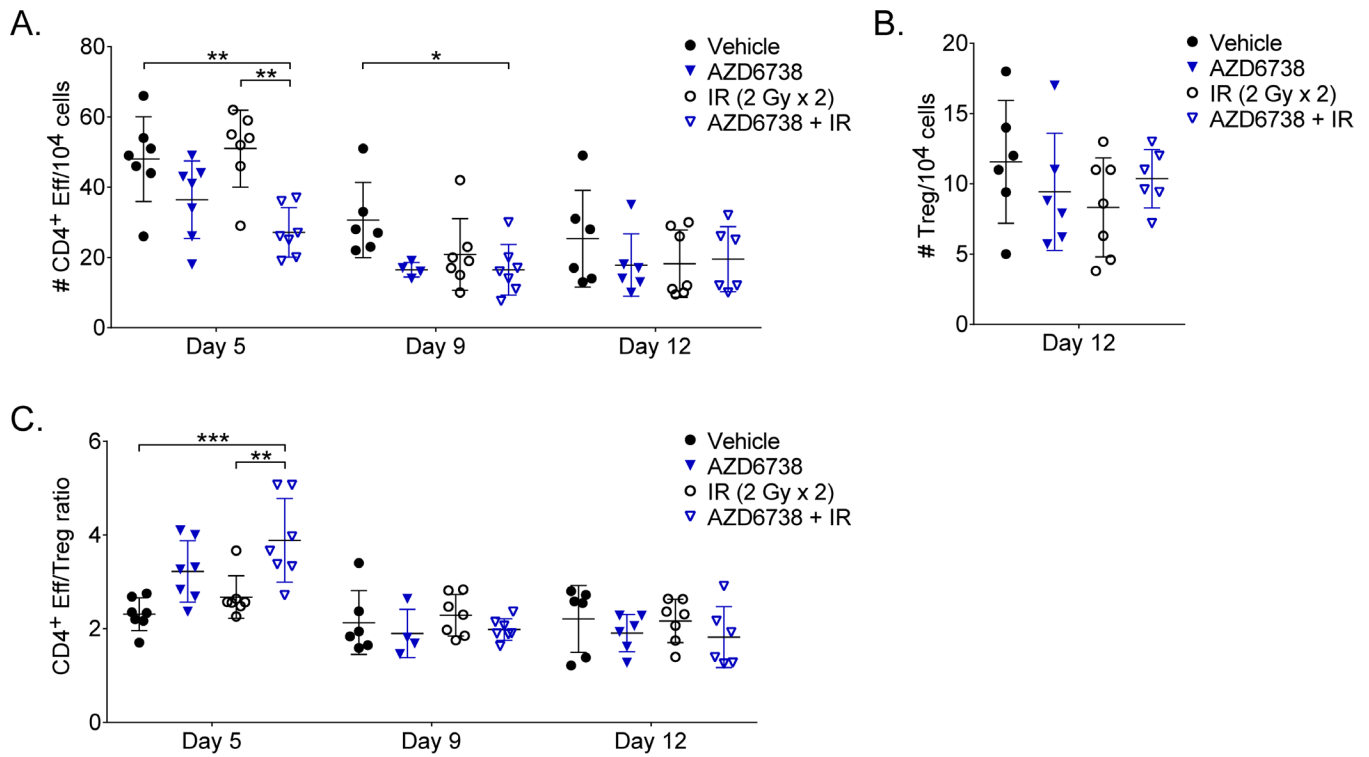
Supplementary Figure S5. Cytokine competency of CT26 tumor-infiltrating T cells at day 5 following treatment with AZD6738 and radiation.

A. Quantitation of the percentages of tumor-infiltrating CD4⁺ Eff T cells expressing IFN γ or IFN γ and TNF α following stimulation with PMA/ionomycin at day 5. **B.** Quantitation of the fold-change in IL-2 MFI (compared to unstimulated spleen control) in tumor-infiltrating CD8⁺ and CD4⁺ Eff T cells following stimulation with PMA/ionomycin at day 5. **A-B.** Data from 3 independent experiments (1 for AZD6738), each with 1-3 mice per arm. n = 6 Vehicle, 3 AZD6738, 5 IR, 5 AZD6738 + IR. Mean and SD bars shown. *p<0.05 by ANOVA with Tukey's multiple comparisons test. Brackets not shown for comparisons that were not statistically significant.



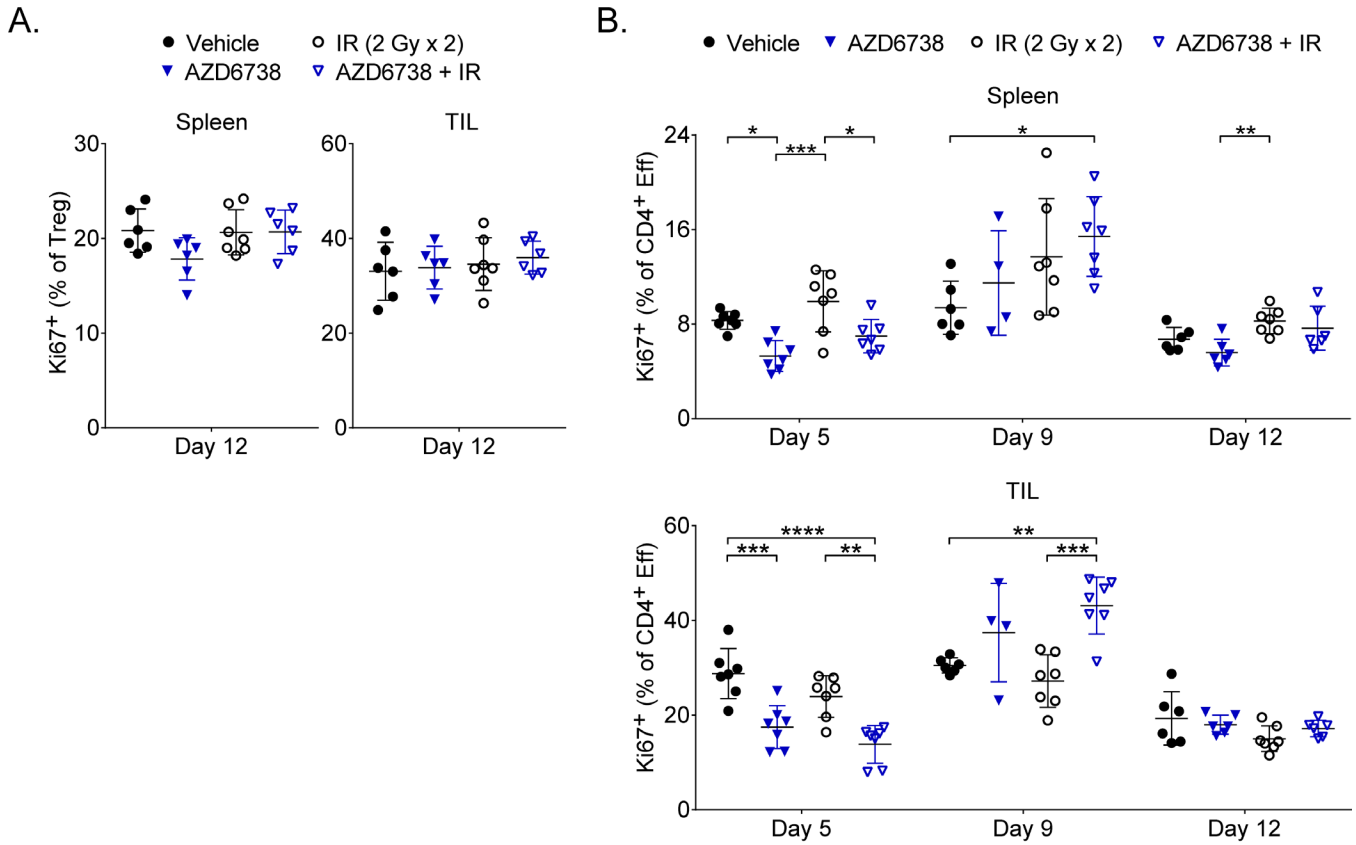
Supplementary Figure S6. PD-L1 knockout CT26 cells are poorly tumorigenic *in vivo*.

A. Histograms demonstrating validation of PD-L1 knockout (KO) CT26 cells by flow cytometry. Positive PD-L1 staining (red) over isotype (black) in wildtype cells is shown for comparison to KO. **B.** Individual growth curves for PD-L1 KO tumors showing tumor volume over time. n = 30 mice injected.



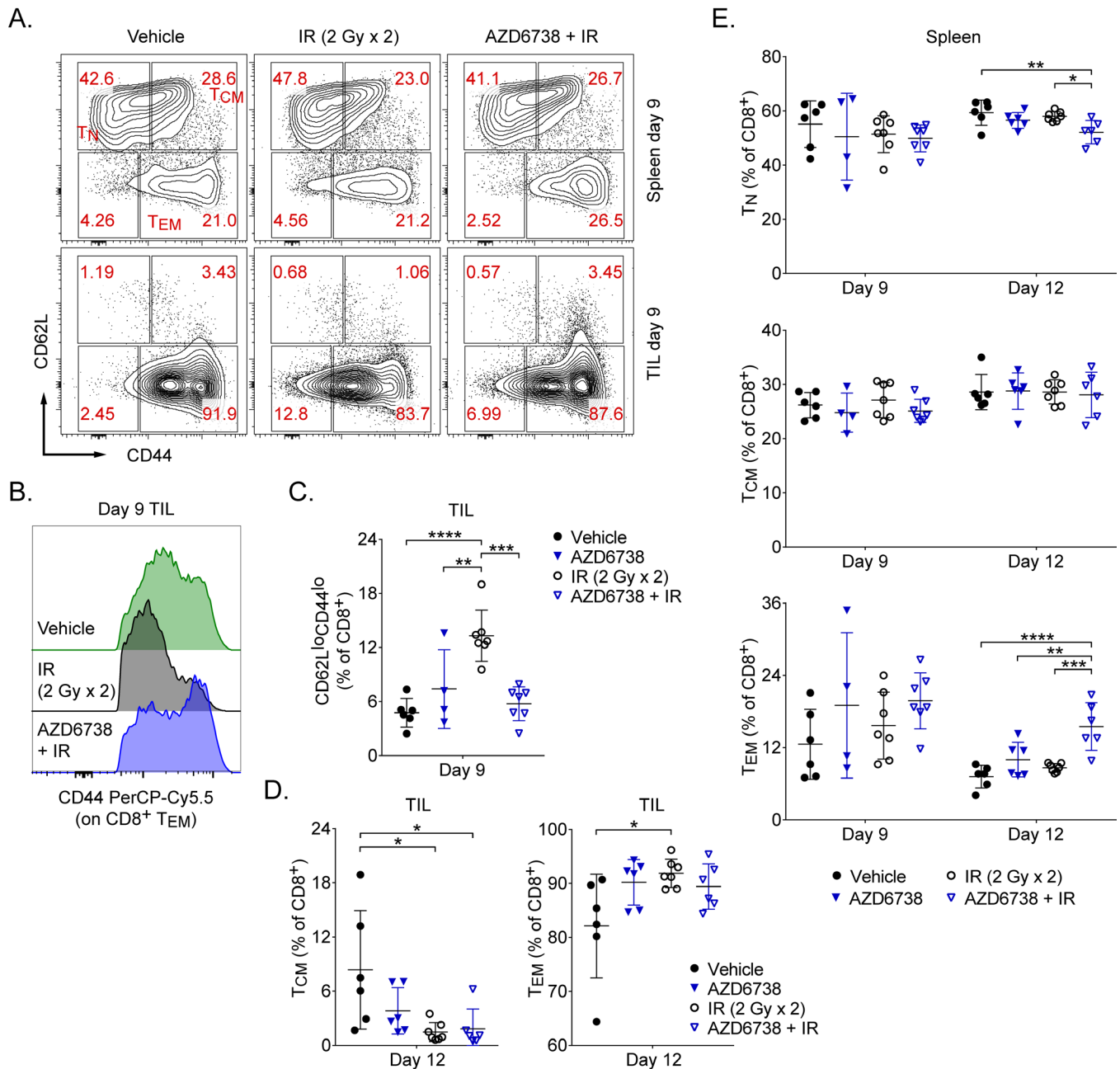
Supplementary Figure S7. T cell infiltration in CT26 tumors following treatment with AZD6738 and radiation.

A. Quantitation of the number of tumor-infiltrating CD4⁺ Eff T cells per 10⁴ cells stained at days 5, 9, and 12. **B.** Quantitation of the number of tumor-infiltrating Treg cells per 10⁴ cells stained at day 12. **C.** CD4⁺ Eff/Treg ratios at days 5, 9, and 12. **A-C.** Data from 3 independent experiments per time point, each with 1-3 mice per arm. n at day 5 = 7 per arm. n at day 9 = 6 Vehicle, 4 AZD6738, 7 IR, 7 AZD6738 + IR. n at day 12 = 6 per arm (7 IR). Mean and SD bars shown. *p < 0.05, **p < 0.01, ***p < 0.001, by ANOVA with Tukey's multiple comparisons test. Brackets not shown for comparisons that were not statistically significant.



Supplementary Figure S8. T cell proliferation in CT26 tumor-bearing mice following treatment with AZD6738 and radiation.

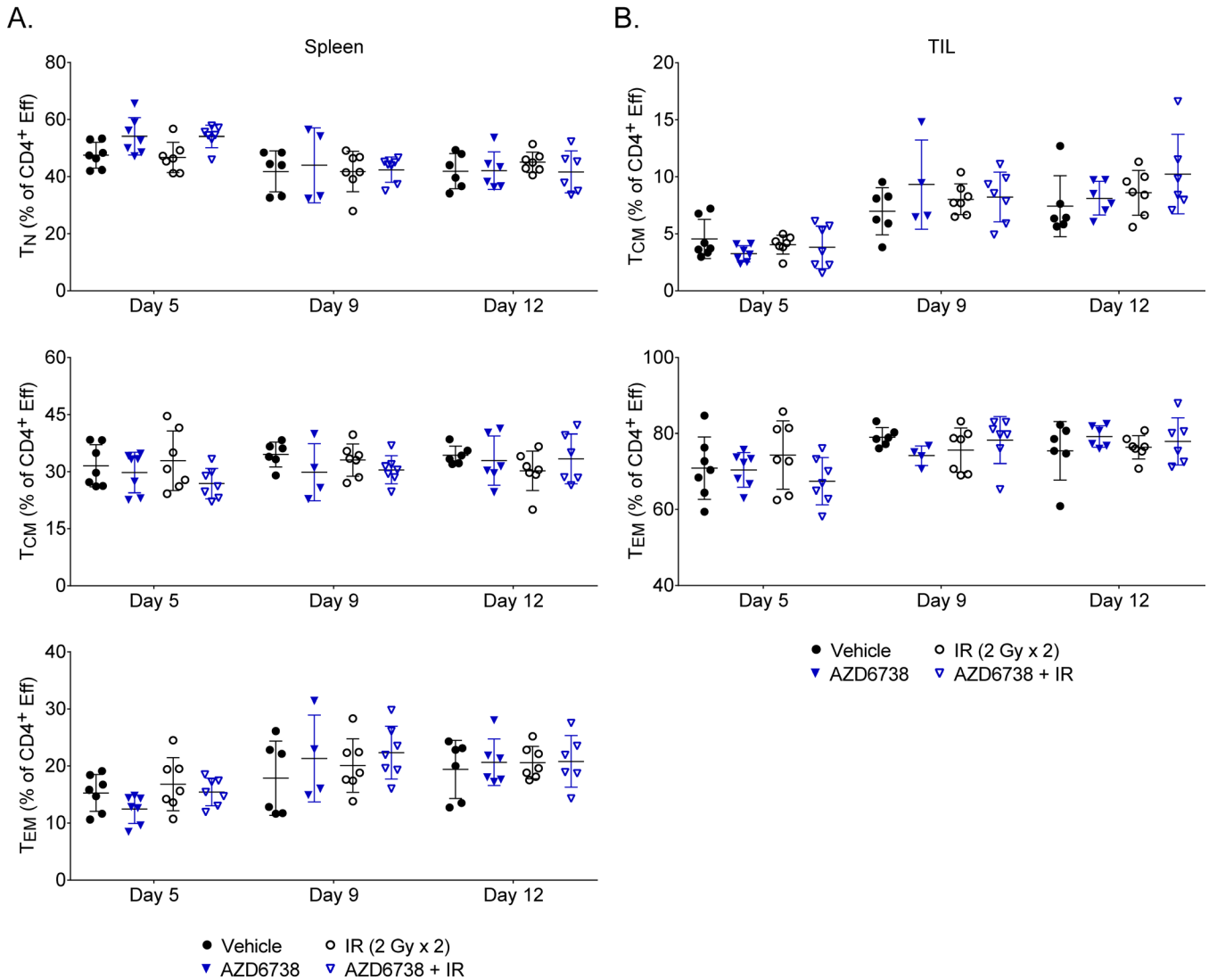
A. Quantitation of the percentage of proliferating (Ki67⁺) splenic and tumor-infiltrating (TIL) Treg cells at day 12. **B.** Quantitation of the percentage of proliferating (Ki67⁺) splenic and TIL CD4⁺ Eff T cells at days 5, 9, and 12. **A-B.** Data from 3 independent experiments per time point, each with 1-3 mice per arm. n at day 5 = 7 per arm. n at day 9 = 6 Vehicle, 4 AZD6738, 7 IR, 7 AZD6738 + IR. n at day 12 = 6 per arm (7 IR). Mean and SD bars shown. *p<0.05, **p<0.01, ***p<0.001, ****p<0.0001 by ANOVA with Tukey's multiple comparisons test. Brackets not shown for comparisons that were not statistically significant.



Supplementary Figure S9. CD8⁺ T cell activation in CT26 tumor-bearing mice following treatment with AZD6738 and radiation.

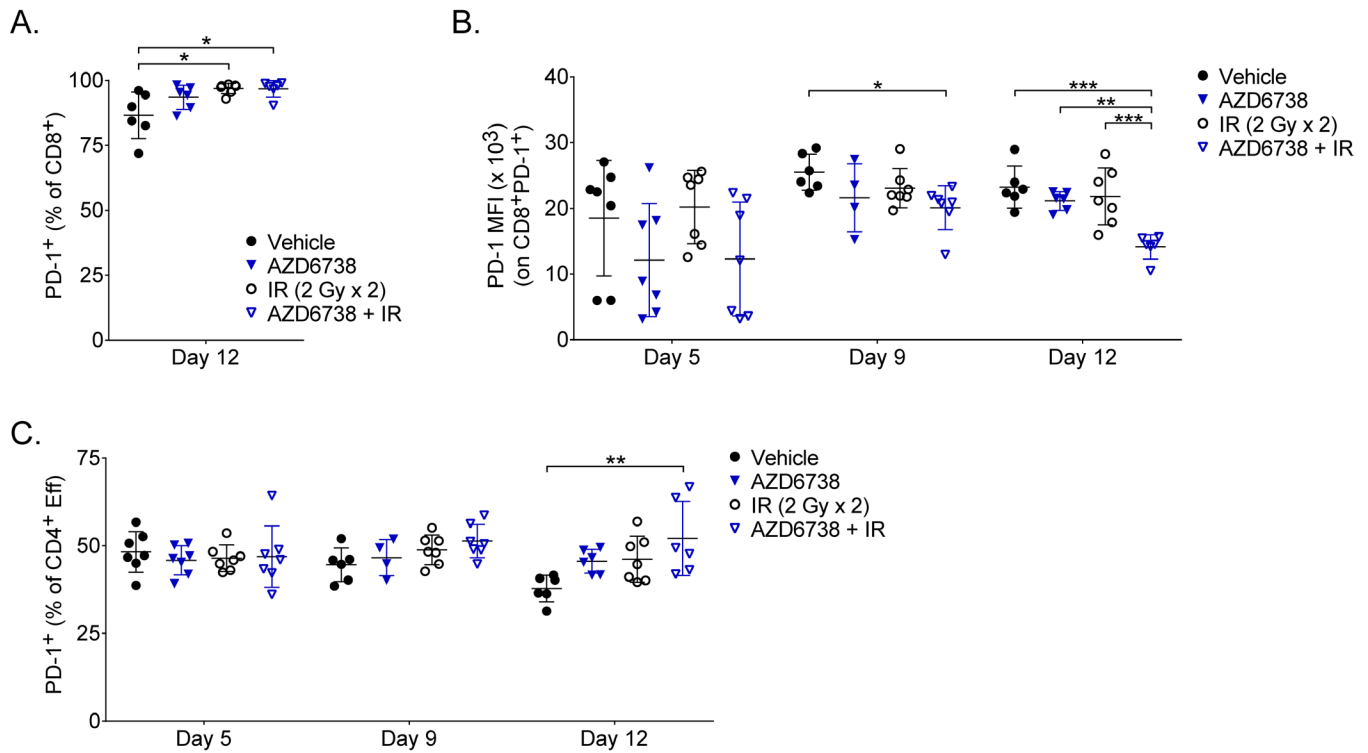
A. Representative contour plots depicting CD62L and CD44 expression on splenic and tumor-infiltrating (TIL) CD8⁺ T cells for the designated treatment groups at day 9. **B.** Quantitation of the percentages of splenic CD8⁺ T cells with naïve (T_N, CD62L^{hi}CD44^{lo}), central memory (T_{CM}, CD62L^{hi}CD44^{hi}), and effector memory (T_{EM}, CD62L^{lo}CD44^{hi}) phenotypes at days 9 and 12. **C.** Representative histograms of CD44 expression on TIL CD8⁺ T_{EM} cells at day 9. **D.** Quantitation of the percentages of TIL CD8⁺ T cells with a CD62L^{lo}CD44^{lo} phenotype at day 9. **E.** Quantitation of the percentages of TIL CD8⁺ T cells with T_{CM} and T_{EM} phenotypes at day 12. **B, D, and E.** Data from 3 independent experiments per time point, each with 1-3 mice per arm. n at day 9 = 6 Vehicle, 4 AZD6738, 7 IR, 7 AZD6738 + IR. n at day 12 = 6 per arm (7

IR). Mean and SD bars shown. * $p < 0.05$, ** $p < 0.01$, *** $p < 0.001$, **** $p < 0.0001$ by ANOVA with Tukey's multiple comparisons test. Brackets not shown for comparisons that were not statistically significant.



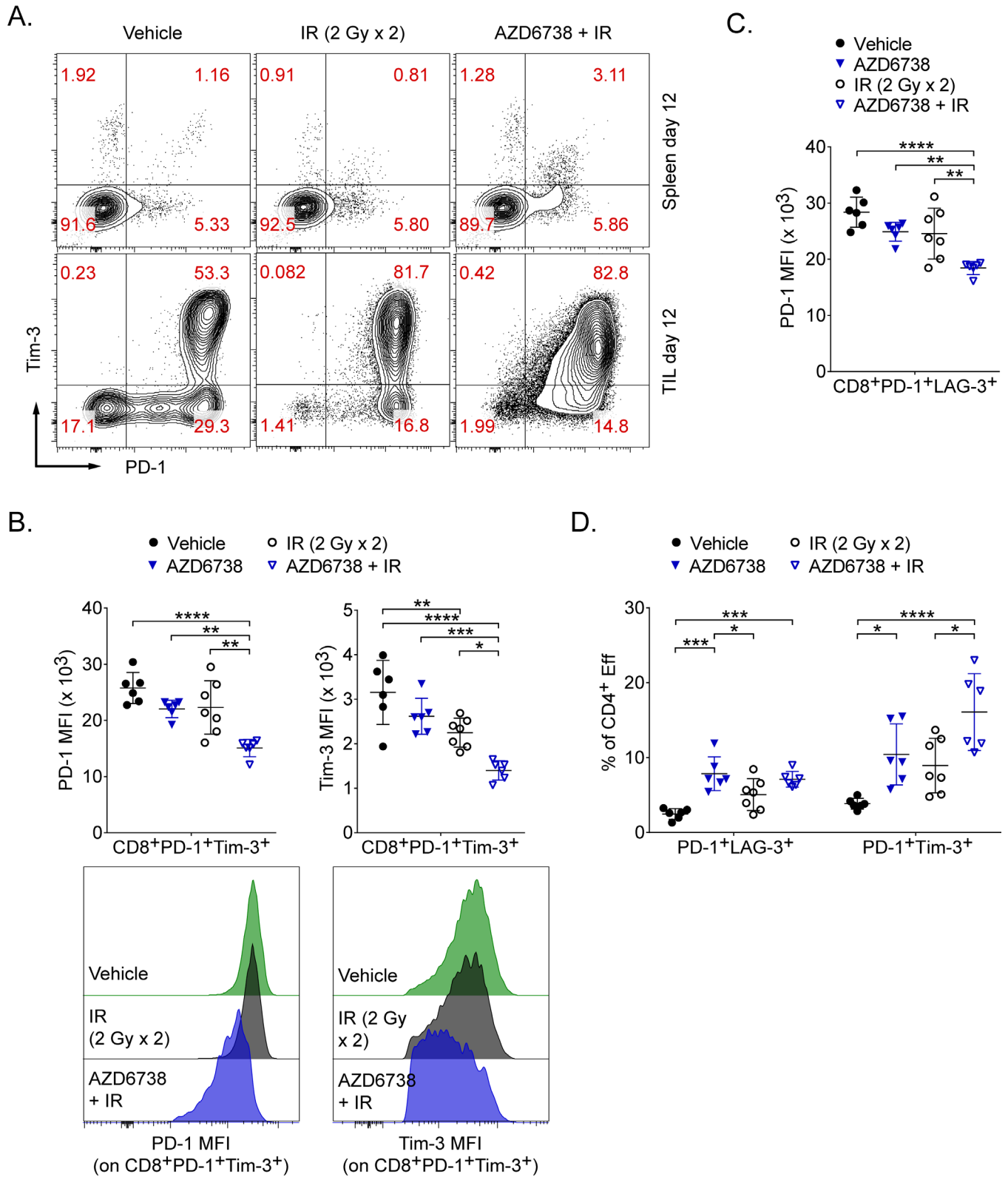
Supplementary Figure S10. CD4⁺ Eff T cell activation in CT26 tumor-bearing mice following treatment with AZD6738 and radiation.

A. Quantitation of the percentages of splenic CD4⁺ Eff T cells with naïve (T_N, CD62L^{hi}CD44^{lo}), central memory (T_{CM}, CD62L^{hi}CD44^{hi}), and effector memory (T_{EM}, CD62L^{lo}CD44^{hi}) phenotypes at days 5, 9, and 12. **B.** Quantitation of the percentages of TIL CD4⁺ Eff T cells with T_{CM} and T_{EM} phenotypes at days 5, 9, and 12. **A-B.** Data from 3 independent experiments per time point, each with 1-3 mice per arm. n at day 5 = 7 per arm. n at day 9 = 6 Vehicle, 4 AZD6738, 7 IR, 7 AZD6738 + IR. n at day 12 = 6 per arm (7 IR). Mean and SD bars shown. ANOVA with Tukey's multiple comparisons test determined no statistically significant differences.



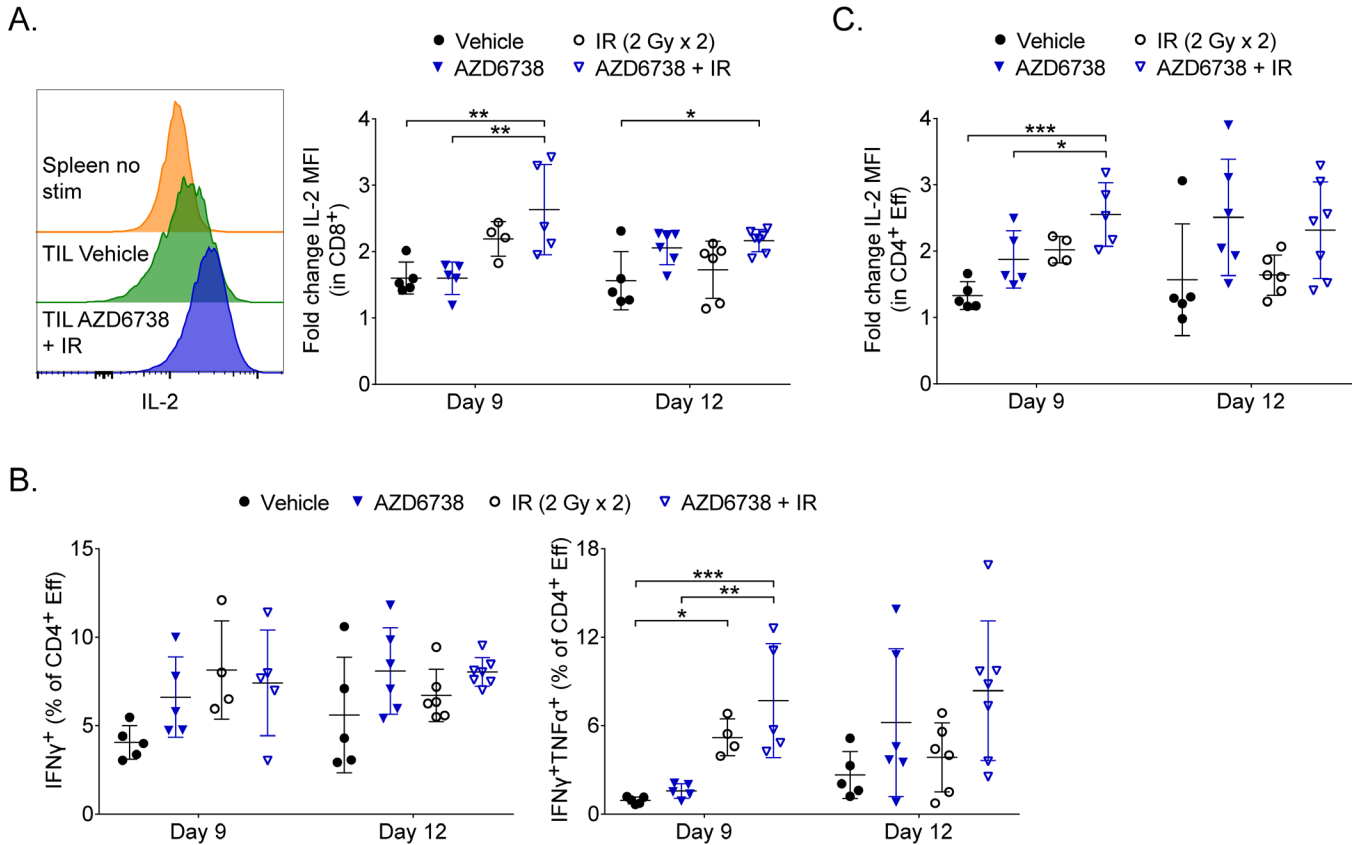
Supplementary Figure S11. Expression of PD-1 on CT26 tumor-infiltrating CD8⁺ and CD4⁺ Eff T cells following treatment with AZD6738 and radiation.

A. Quantitation of the percentages of tumor-infiltrating (TIL) CD8⁺ T cells that express PD-1 at day 12. **B.** Quantitation of the PD-1 median fluorescence intensity (MFI) on TIL CD8⁺PD-1⁺ T cells at days 5, 9, and 12. **C.** Quantitation of the percentages of tumor-infiltrating (TIL) CD4⁺ Eff T cells that express PD-1 at days 5, 9, and 12. **A-C.** Data from 3 independent experiments per time point, each with 1-3 mice per arm. n at day 5 = 7 per arm. n at day 9 = 6 Vehicle, 4 AZD6738, 7 IR, 7 AZD6738 + IR. n at day 12 = 6 per arm (7 IR). Mean and SD bars shown. *p<0.05, **p<0.01, ***p<0.001 by ANOVA with Tukey's multiple comparisons test. Brackets not shown for comparisons that were not statistically significant.



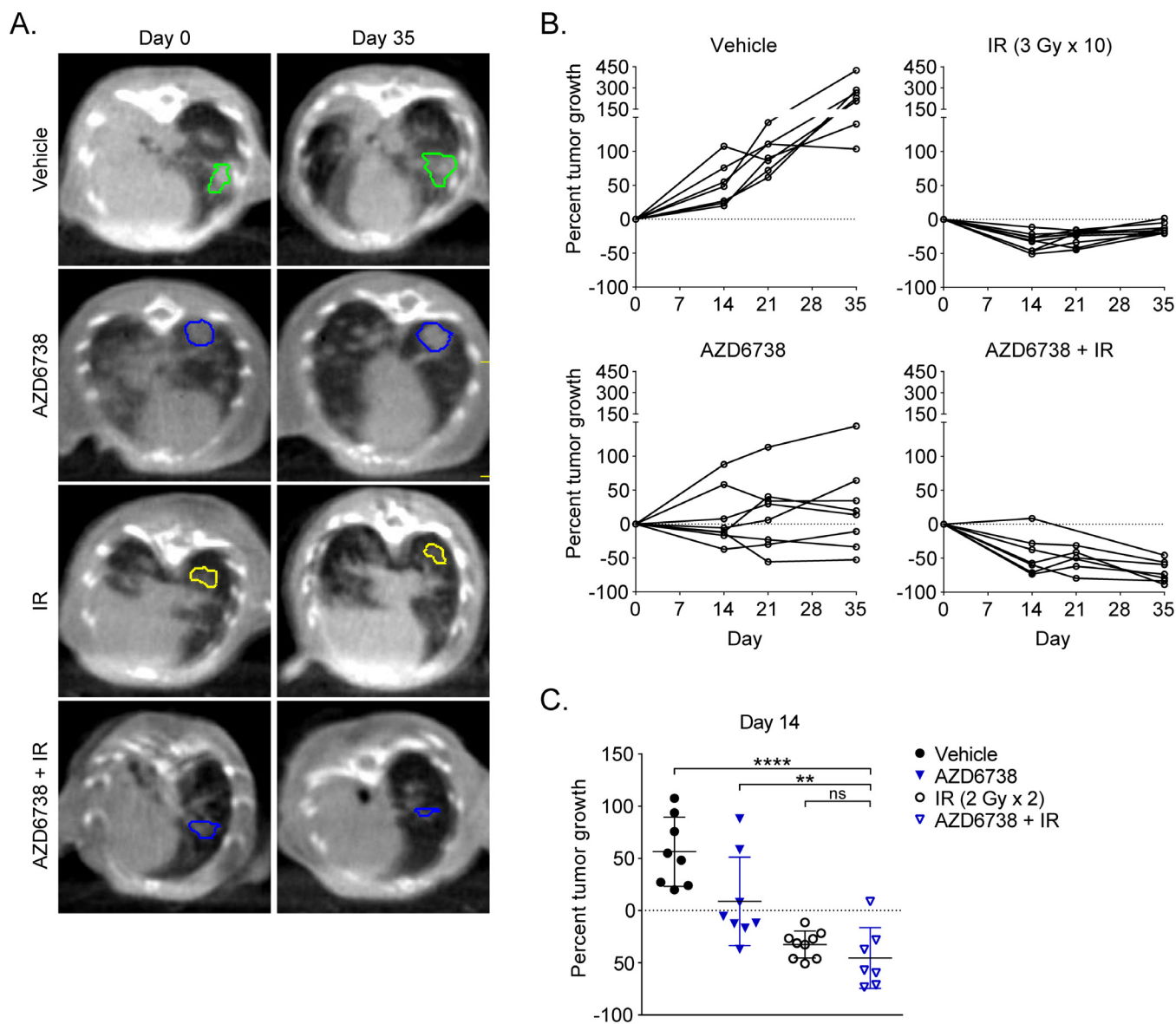
Supplementary Figure S12. Expression of T cell exhaustion markers on CT26 tumor-infiltrating CD8⁺ and CD4⁺ Eff T cells following treatment with AZD6738 and radiation.

A. Representative contour plots depicting PD-1 and Tim-3 expression on spleen and TIL CD8⁺ T cells for the designated treatment groups at day 12. **B.** Quantitation of the median fluorescence intensity (MFI) of PD-1 or Tim-3 on TIL CD8⁺PD-1⁺Tim-3⁺ T cells at day 12 with corresponding representative histograms of PD-1 or Tim-3 expression below. **C.** Quantitation of the median fluorescence intensity (MFI) of PD-1 on TIL CD8⁺PD-1⁺LAG-3⁺ T cells at day 12. **D.** Quantitation of the percentages of tumor-infiltrating (TIL) CD4⁺ Eff T cells that co-express PD-1 and LAG-3 or PD-1 and Tim-3 at day 12. **B-D.** Data from 3 independent experiments, each with 1-3 mice per arm. n at day 12 = 6 per arm (7 IR). Mean and SD bars shown. *p<0.05, **p<0.01, ***p<0.001, ****p<0.0001 by ANOVA with Tukey's multiple comparisons test. Brackets not shown for comparisons that were not statistically significant.



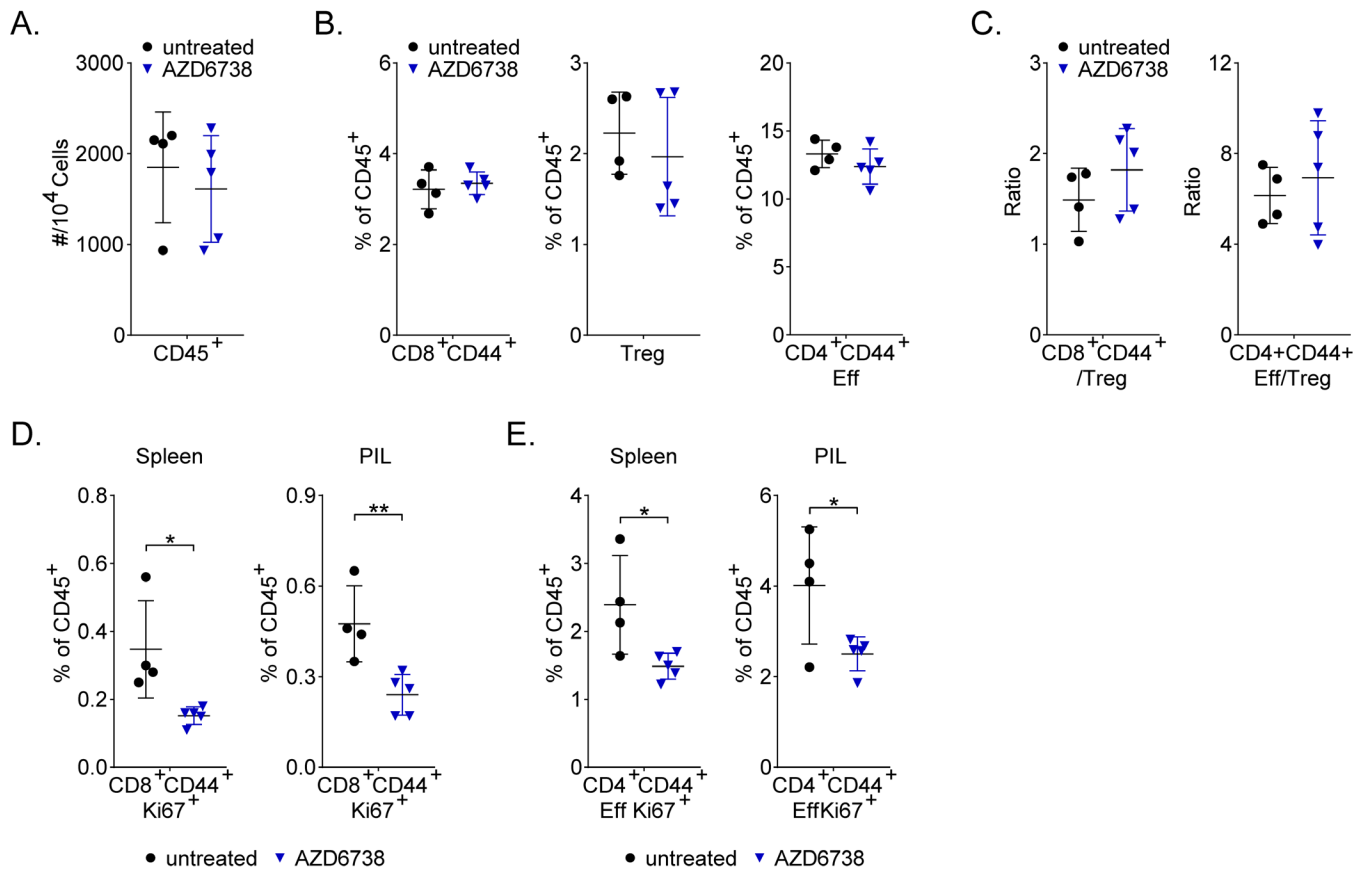
Supplementary Figure S13. Cytokine competency of CT26 tumor-infiltrating T cells following treatment with AZD6738 and radiation.

A. Representative histograms of IL-2 expression in tumor-infiltrating CD8⁺ T cells at day 12 for the designated treatments and corresponding quantitation of the fold-change in IL-2 MFI (compared to unstimulated spleen control) following stimulation with PMA/ionomycin at days 9 and 12. **B.** Quantitation of the percentages of tumor-infiltrating CD4⁺ Eff T cells that elicit IFN γ or IFN γ and TNF α following stimulation with PMA/ionomycin at days 9 and 12. **C.** Quantitation of the fold-change in IL-2 MFI (compared to unstimulated spleen control) in tumor-infiltrating CD4⁺ Eff T cells following stimulation with PMA/ionomycin at days 9 and 12. **A-C.** Day 9 data from one experiment with the IR/AZD6738 + IR arms and Vehicle/AZD6738 arms staggered and harvested/stained on separate days. n at day 9 = 5 per arm (4 IR). Day 12 data from 3 independent experiments, each with 1-3 mice per arm, with harvesting/staining for all arms performed on the same day within a given experiment. n at day 12 = 5 Vehicle, 6 AZD6738, 6 IR, 7 AZD6738 + IR. Mean and SD bars shown. *p<0.05, **p<0.01, ***p<0.001 by ANOVA with Tukey's multiple comparisons test. Brackets not shown for comparisons that were not statistically significant.



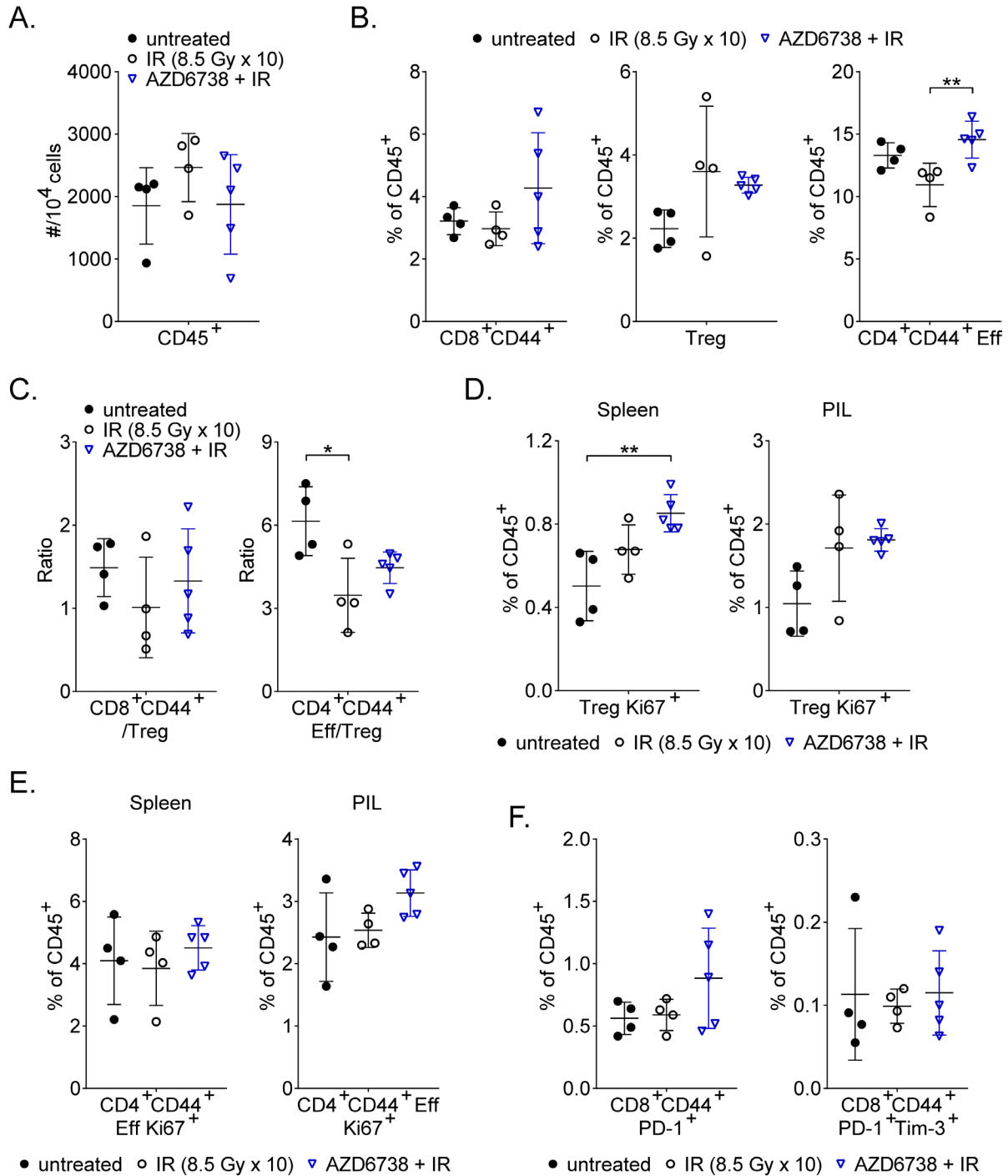
Supplementary Figure S14. AZD6738 radiosensitizes *Kras*^{G12D}/*Twist1* lung adenocarcinoma

A. Representative micro-CT images at day 0 and day 35 depicting lung tumors (encircled) in mice treated with Vehicle, AZD6738, IR, or AZD6738 + IR. **B.** Response of individual lung tumors over time, represented as the percent change in tumor volume from day 0 at each time point. n (tumors/mice) = 7/3 Vehicle, 8/4 AZD6738, 9/4 IR, 7/4 AZD6738 + IR (5/3 day 21). **C.** Percent change in lung tumor volume at day 14 (compared to day 0). n (tumors/mice) = 8/3 Vehicle, 8/4 AZD6738, 9/4 IR, 7/4 AZD6738 + IR. The additional tumor quantified in the Vehicle treatment arm at this timepoint (not included in panel B) was not quantifiable at later timepoints due to a collapsed lung. Mean and SD bars shown. ** $p < 0.01$, **** $p < 0.0001$ by ANOVA with Holm-Sidak's multiple comparisons test. ns = not significant. Statistical significance shown only for comparisons with AZD6738 + IR, denoted with brackets.



Supplementary Figure S15. Immune profiling of splenic and pulmonary-infiltrating T cells in *Kras*^{G12D}/*Twist1* lung adenocarcinoma-bearing mice at day 5 following treatment with AZD6738.

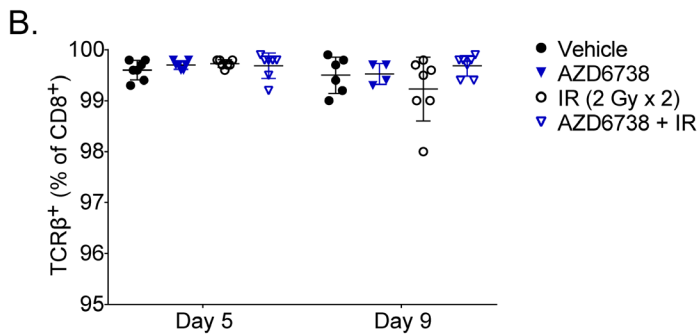
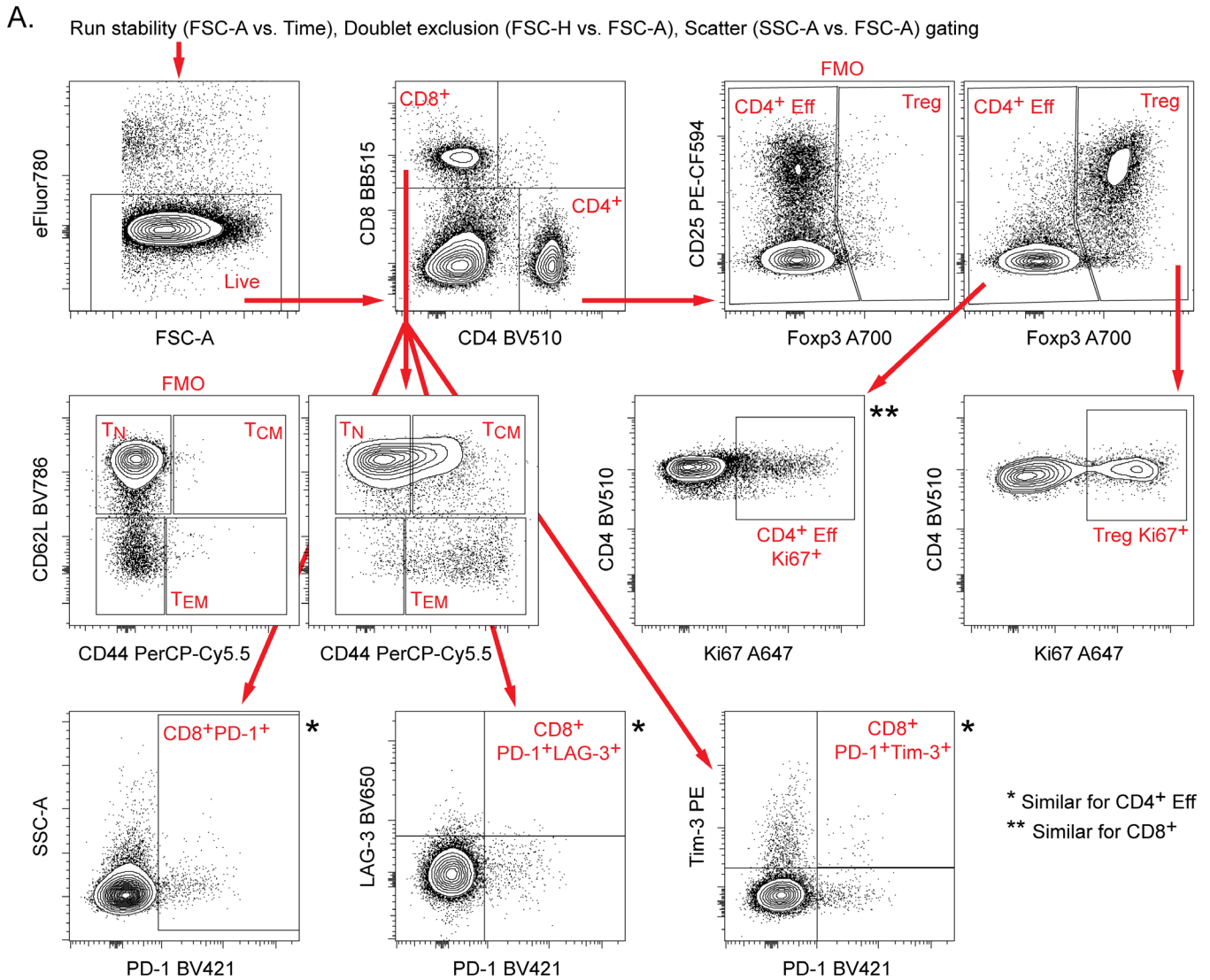
A. Quantitation of the number of pulmonary-infiltrating CD45⁺ immune cells (per 10⁴ cells stained). **B.** Quantitation (as a percentage of CD45⁺ immune cells) of pulmonary-infiltrating activated CD8⁺CD44⁺ T cells, Treg cells, and activated CD4⁺CD44⁺ Eff T cells. **C.** Pulmonary-infiltrating CD8⁺CD44⁺/Treg and CD4⁺CD44⁺ Eff/Treg ratios. **D.** Quantitation of splenic and pulmonary-infiltrating (PIL) proliferating (Ki67⁺) CD8⁺CD44⁺ T cells. **E.** Quantitation of splenic and PIL proliferating (Ki67⁺) CD4⁺CD44⁺ Eff T cells. **A-E.** Data from 2 (AZD6738) or 3 (untreated control) independent experiments, with 1-4 mice per arm per experiment. n = 4 untreated control, 5 AZD6738. Mean and SD bars shown. *p<0.05, **p<0.01 unpaired, two-tailed t test. Brackets not shown for comparisons that were not statistically significant.



Supplementary Figure S16. Immune profiling of splenic and pulmonary-infiltrating T cells in *Kras*^{G12D}/*Twist1* lung adenocarcinoma-bearing mice at day 9 following treatment with AZD6738 and radiation.

A. Quantitation of the number of pulmonary-infiltrating CD45⁺ immune cells (per 10⁴ cells stained). **B.** Quantitation (as a percentage of CD45⁺ immune cells) of pulmonary-infiltrating activated CD8⁺CD44⁺ T cells, Treg cells, and activated CD4⁺CD44⁺ Eff T cells. **C.** Pulmonary-infiltrating CD8⁺CD44⁺/Treg and CD4⁺CD44⁺ Eff/Treg ratios. **D.** Quantitation of splenic and pulmonary-infiltrating (PIL) proliferating (Ki67⁺)

Treg cells. **E.** Quantitation of splenic and PIL proliferating (Ki67⁺) CD4⁺CD44⁺ Eff T cells. **F.** Quantitation of pulmonary-infiltrating CD8⁺CD44⁺ T cells that express PD-1 (CD8⁺CD44⁺PD-1⁺) and CD8⁺CD44⁺ T cells that co-express PD-1 and Tim-3 (CD8⁺CD44⁺PD-1⁺Tim-3⁺). **A-F.** Data from 1 (IR and AZD6738 + IR) or 3 (untreated control) independent experiments, with 1-5 mice per arm per experiment. n = 4 untreated control, 4 IR, 5 AZD6738 + IR. Mean and SD bars shown. *p<0.05, **p<0.01 by ANOVA with Tukey's multiple comparisons test. Brackets not shown for comparisons that were not statistically significant.

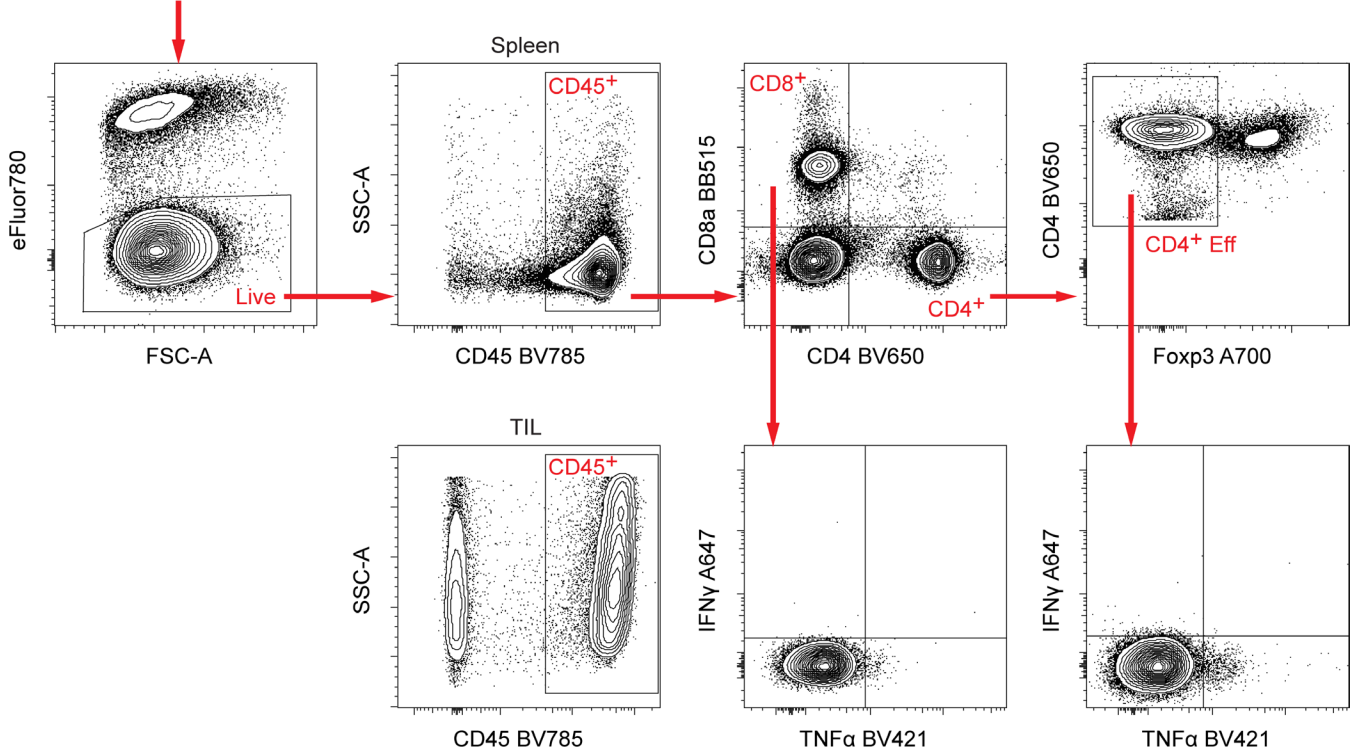


Supplementary Figure S17. Gating strategy for immune profiling of splenic and tumor-infiltrating T cell populations in CT26 tumor-bearing mice.

A. Following exclusion of unstable portions of the run and doublets, cells were gated based on SSC-A and FSC-A characteristics, followed by gating for live cells (eFluor780^{neg}) prior to downstream analyses as shown. CD4⁺ cells were characterized as CD4⁺ Eff T cells (Foxp3^{neg}) or Treg (Foxp3⁺). Within the

CD8⁺ and CD4⁺ Eff T cell populations, cells were characterized as naïve (T_N, CD62L^{hi}CD44^{lo}), central memory (T_{CM}, CD62L^{hi}CD44^{hi}), and effector memory (T_{EM}, CD62L^{lo}CD44^{hi}) populations. Expression of PD-1, LAG-3 (day 12 only), and Tim-3 (day 12 only) were also examined on CD8⁺ and CD4⁺ Eff T cells. Expression of Ki67 was examined in the CD8⁺, CD4⁺ Eff, and Treg populations. Gates were established using spleens of Vehicle control mice, and FMO controls (where appropriate). Example FMO controls are shown for Foxp3 and CD44. **B.** Quantitation of tumor-infiltrating TCRβ⁺CD8⁺ T cells in the CD8 gate at day 5 and day 9. Anti-TCRβ PE-Cy7 antibody was included in the staining panel for all day 5 and day 9 experiments. Nearly all (≥ 99%, with 1 sample ≥ 98%) of the tumor-infiltrating CD8⁺ cells were also TCRβ⁺ (n = 52 mice from 6 independent experiments across the two time points). As tumor-infiltrating CD8⁺ T cells were the primary population of focus, and gating for Treg included additional identifying markers, anti-TCRβ antibody was omitted from other experiments to reduce compensation requirements and data spreading. For consistency with other experiments, TCRβ was excluded from the gating strategy and downstream analyses for all day 5 and day 9 CT26 T cell immune profiling experiments.

Run stability (FSC-A vs. Time), Doublet exclusion (FSC-H vs. FSC-A), Scatter (SSC-A vs. FSC-A) gating



Supplementary Figure S18. Gating strategy for analysis of tumor-infiltrating T cell cytokine competency in CT26 tumor-bearing mice.

Following exclusion of unstable portions of the run and doublets, cells were gated based on SSC-A and FSC-A characteristics, followed by gating for live cells (eFluor780^{neg}) prior to downstream analyses as shown. CD4⁺ Eff cells were further characterized as FcγR3^{neg}. Within the CD8⁺ and CD4⁺ Eff T cell populations, cells were characterized for expression of IFNγ and TNFα, as well as the median fluorescence intensity (MFI) of IL-2 expression (not shown). Gates were established using unstimulated spleen controls, as shown. Gating on CD45⁺ cells from unstimulated TIL (tumor-infiltrating lymphocytes) control shown for comparison.

Supplemental References

1. Kiesel BF, Shogan JC, Rachid M, Parise RA, Vendetti FP, Bakkenist CJ, and Beumer JH. LC-MS/MS assay for the simultaneous quantitation of the ATM inhibitor AZ31 and the ATR inhibitor AZD6738 in mouse plasma. *J Pharm Biomed Anal.* 2017;138(158-65).